Geomechanics and Engineering, *Vol. 24, No. 6 (2021) 599-610*
DOI: https://doi.org/10.12989/gae.2021.24.6.599

Vertical load on a conduit buried under a sloping ground

Muhammad U. A. Khan*[1,2] and Sanjay K. Shukla[1,3a]

[1]*Geotechnical and Geoenvironmental Engineering Research Group, School of Engineering, Edith Cowan University, WA 6027, Australia*
[2]*Department of Civil Engineering, Mirpur University of Science and Technology, Mirpur, Azad Kashmir, Pakistan*
[3]*Department of Civil Engineering, Delhi Technological University, Delhi, India*

(Received January 14, 2020, Revised March 17, 2021, Accepted March 19, 2021)

Abstract. Conduits are commonly installed below the ground for utility conveyance around the world. Vertical load on a buried conduit is an important parameter that needs to be known to ensure its safe design and installation. Consideration of soil arching in load calculations helps achieve a more realistic and efficient design. In the past, considering the arching effect, the design charts have been presented for use by practicing engineers to calculate the vertical load on the conduit buried below the level ground. There are currently no design charts for calculating the vertical load on the conduit buried under a sloping ground. In this paper, an attempt has been made to present the derivation of a generalized analytical expression considering that the soil mass overlying the conduit has a sloping face and the arching phenomenon takes place. The developed generalized expression has been used to present some design charts considering specific values of slope geometry, soil properties and burial depths. Furthermore, analytical results for specific soil parameters have been compared with the results extracted from a commercial software PLAXIS 2D, for a developed numerical model and an independent study.

Keywords: arching; finite element analysis; sloping ground; soil-conduit interaction; vertical load

1. Introduction

In many countries, the task of infrastructure development is challenging due to hilly terrain. Considering the economic and safety benefits, buried conduits have become the primary source of conveying services, such as water, gas, electrical cable, etc. The presence of buried conduits in hilly slopes is very common (Uchida 2004). The design of buried conduits depends on the external load applied by the overburden soil and the surface surcharge. To-date, many researchers have used various experimental and numerical methods to understand the soil-conduit interaction (Dhar *et al.* 2004, Srivastava and Babu 2011, Talesnick *et al.* 2011, Bryden *et al.* 2015, Khatri *et al.* 2015, Terzi *et al.* 2015, Allard and Naggar 2016, Mohamedzein and Al-Aghbari 2016, Katona 2017, Alzabeebee *et al.* 2018, Khan and Shukla 2020). While studying the soil-conduit interaction, soil arching is one of the most frequently encountered phenomena (Terzaghi 1943). Arching takes place when the stress over a yielding mass is transferred to the adjacent stationary soil, resulting in reduced pressure on the yielding mass (Marston 1930, Terzaghi 1943). Numerous studies regarding the arching phenomenon can be found in the present literature (Sardrekarimi and Abbasnejad 2010, Ting *et al.* 2011, Kim *et al.* 2013, Moradi and Abbasnejad 2015, Lee *et al.* 2016, Xu *et al.* 2019). Consideration of the arching action in calculation of the vertical load on the buried conduit helps achieve a more efficient design (Moser and Folkman 2001). Depending upon the stiffness of the conduit material, the load on the buried conduit increases or decreases, resulting in negative or positive arching, respectively (Moore 2001, Kang *et al.* 2008). Some classical arching theories have also been used to explain the arching phenomenon. Nielson (1966) and Lucher and Hoeg (1964) studied arching under static loading conditions, by considering soil on top of the conduit to be an arch or a dome. The elastic theory was also employed to study arching and its effect on the vertical load transferred to the buried conduits by several researchers (Chelapati 1964, Bjerrum *et al.* 1972, Burghignoli 1981).

Marston and Anderson (1913) and Terzaghi (1943) used the shear plane method for load estimation on buried conduits. This method is based on an internal soil prism located above the buried conduit that yields with respect to the adjoining soil mass. Vertical shear planes separate the yielding soil prism from the adjoining soil mass. The frictional resistance acting along the shear planes reduces the load of the yielding soil prism on the buried conduit. The load of the soil prism taken by the buried conduit depends on its stiffness (Spangler 1962, Greenwood and Lang 1990). For a rigid conduit, the entire load of the soil prism is taken by the buried conduit; whereas, for a flexible conduit, the load of the soil prism is uniformly spread over the entire width of the soil prism (Spangler 1962, Spangler and Handy 1973). Spangler (1962) presented the following expressions for vertical load W transferred to the conduit buried under cohesionless soil with zero surface surcharge.
For rigid conduit

$$W = C_d \gamma B^2 \tag{1}$$

*Corresponding author, Ph.D. Candidate
E-mail: umer.arif1@gmail.com
[a]Founding Research Group Leader
E-mail: s.shukla@ecu.edu.au, sanjaykshukla1@gmail.com

ISSN: 2005-307X (Print), 2092-6219 (Online)

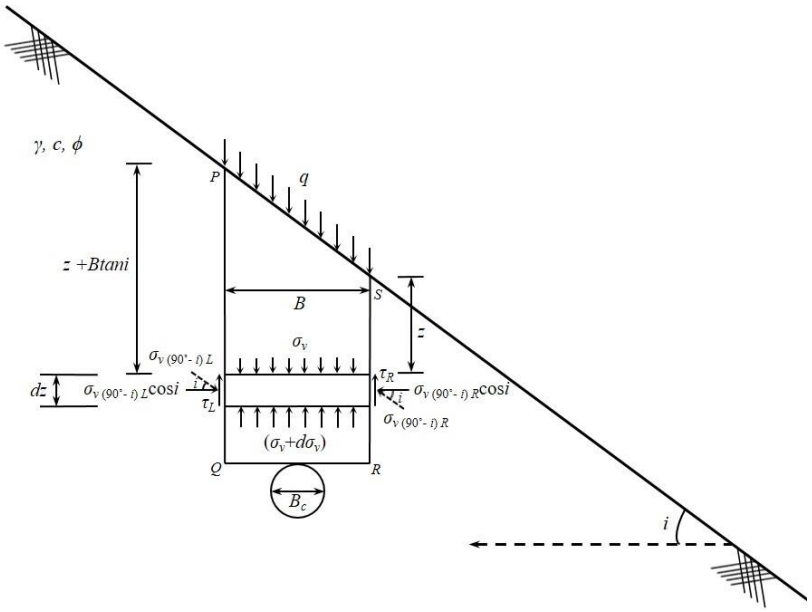

Fig. 1 Yielding soil prism over the conduit buried under the sloping ground

For a flexible conduit, the vertical load W is given by multiplying Eq. (1) with B_c/B

$$W = C_d \gamma B B_c \tag{2}$$

where C_d is the load coefficient, expressed as

$$C_d = \frac{1}{2K\mu}\left(1 - e^{-2K\mu\frac{z}{B}}\right) \tag{3}$$

where γ is the total unit weight of soil, B is the width of yielding soil prism, B_c is the outside diameter of the buried conduit, z is the depth of buried conduit from the level ground, K is the lateral stress ratio, and μ=tanϕ is the friction coefficient (where ϕ represents the angle of internal friction of soil lying over the conduit).

Eqs. (1) and (2) are frequently used for an efficient design of the conduit buried under a level ground. There is currently no analytical expression available for estimation of vertical load on the conduit buried under a sloping ground. However, it needs to be noted that Wadi *et al.* (2015) conducted a numerical study using the commercial software, PLAXIS 2D, to understand the structural behavior of corrugated steel (CS) pipe culverts buried at different depths under a sloping ground. Considering the limited scope of their work that requires access to expensive commercial software, there is a need for a simple analytical solution that can be used more frequently by practicing engineers. Therefore, in this paper, an attempt has been made to develop an analytical expression and present the design charts for estimation of vertical load on both rigid and flexible conduits buried under the sloping ground.

2. Analytical formulation

Considering the arching phenomenon, Marston and Anderson (1913) and Terzaghi (1943) provided the analytical formulation for calculating the vertical load on a conduit buried under the level ground, considering the following assumptions;

a) The entire soil mass is homogeneous.

b) The lateral stress ratio is constant at every point in the soil mass and is suggested as the active Rankine ratio.

c) The vertical stresses on the horizontal yielding surface are uniform.

d) Shear failure only occurs along the vertical shear planes.

e) The conduit is buried under the natural ground surface i.e., the ditch condition and has more stiffness than the adjoining soil mass.

Considering these assumptions, unless otherwise noted, the analytical expression to calculate the load on a conduit buried under a sloping ground has been derived, as explained below.

Fig. 1 shows a rigid conduit of external diameter B_c, buried under a sloping ground inclined at an angle i with the horizontal. The entire soil mass of the sloping ground has a total unit weight γ, cohesion c and angle of internal friction ϕ. The surface of the soil carries a uniform surface surcharge q per unit area. The soil prism $PQRS$ of width B yields with respect to the adjoining soil, separated by vertical shear planes PQ and RS. The arching phenomenon occurs due to the frictional resistance acting along the vertical shear planes. Because of the higher stiffness of the conduit relative to the adjacent soil, the buried conduit takes the entire load of the yielding soil prism $PQRS$.

In order to understand the arching effect, a horizontal differential strip of thickness dz is considered. Along the shear planes PQ and RS, depths of the differential strip from the slope surface are z+Btan$i$ and z, respectively. Forces acting on the differential strip are shown in Fig. 2.

In Fig. 2, the area of strip A_{strip} is expressed as

$$A_{strip} = Bdz \tag{4}$$

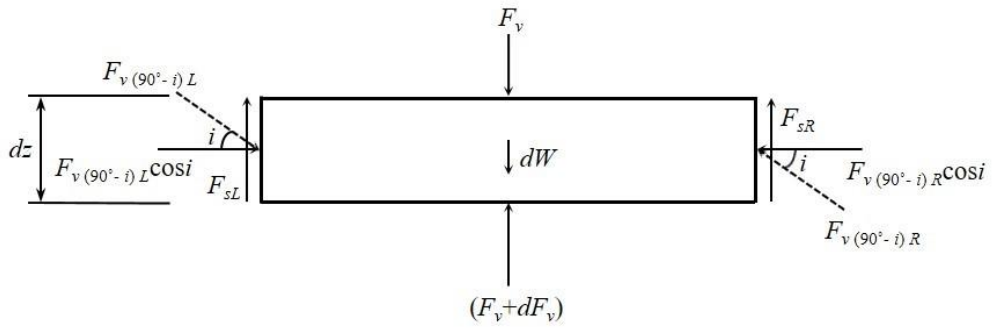

Fig. 2 Forces acting on the differential soil strip

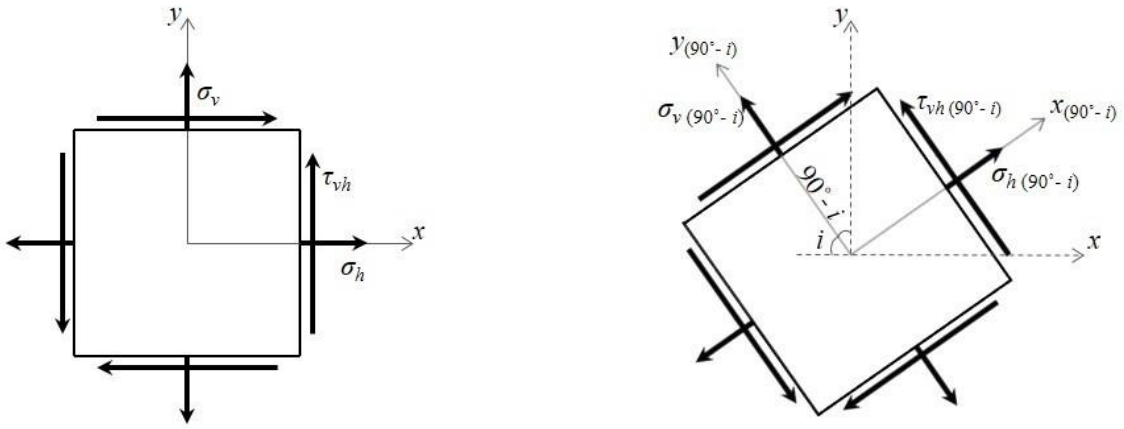

(a) Defined along vertical and horizontal planes (b) Oriented at an angle (90˚–*i*) with vertical axis

Fig. 3 Stresses on the soil element

The self-weight dW of the strip is obtained as

$$dW = \gamma B dz \tag{5}$$

The force F_v on top of the strip at depth z is given as

$$F_v = \sigma_v B \tag{6}$$

where σ_v is the average intensity of overburden stress spread over width B at a depth z.

The force F_v+dF_v on the bottom of the strip is given as

$$F_v + dF_v = (\sigma_v + d\sigma_v)B \tag{7}$$

Like any other material, stresses normal to a point within the soil mass exist in every direction and can only be defined in terms of the orientation of the assumed plane passing through the point. It is, therefore meaningless to talk about normal stress at a point without defining the orientation of the assumed plane (Lambe and Whitman 1969). For example, while studying the lateral earth pressure on a retaining wall for a sloping ground, the vertical stress σ_v at a point at the depth z, on a plane parallel to the sloping surface inclined at an angle i to the horizontal is given as $\sigma_v=\gamma z\cos i$ (Aysen 2002). However, if the orientation of the assumed plane is changed to horizontal (i.e., i=0˚), the vertical stress equals $\sigma_v=\gamma z$. This is the same value of the vertical stress σ_v, at a point under a level ground at the depth z, when the orientation of the plane is taken as horizontal. This confirms that the stress at a point within a soil mass is independent of the inclination of the ground surface, rather its value depends on the orientation of the plane used to define it. Fig. 3(a) shows the stresses on a soil element when the assumed planes are defined as vertical and horizontal i.e., along xy coordinates. Using the above-stated concept, along the shear plane RS, the value of the vertical stress σ_v at a depth z is given as

$$\sigma_v = \gamma z \tag{8}$$

The horizontal stress σ_h can be calculated by multiplying the vertical stress σ_v with the lateral stress ratio K,

$$\sigma_h = K\sigma_v \tag{9}$$

Assuming that the Coulomb's strength principle is appropriate for the slope material, the shear force τ_{vh} acting on the element is given as

$$\tau_{vh} = c + K\sigma_v \tan\phi \tag{10}$$

where c is the soil cohesion.

It needs to be noted here that among all the planes that can be used to define the value of normal stress, only one is the principal plane. In a homogeneous soil mass, where the nature of soil varies but little in the horizontal direction (i.e., i=0˚), a point within the soil mass is under the geostatic stress condition with principal stresses acting

along vertical and horizontal planes. However, in the case of a sloping ground, the principal stresses acting at a point are no longer vertical and horizontal, but are inclined along the potential slip surface of the slope (Wu 1996, Xiao *et al.* 2011). For an infinite soil slope, the potential slip surface is assumed to be parallel to the sloping surface (Atkinson 2007, Lambe and Whitman 1969). In such cases, the known stresses acting along the vertical and horizontal planes can be used to calculate the stresses on the inclined plane, by applying the concept of stress transformation (Young *et al.* 2002, Das 2008).

By employing the above-stated concept, the soil element shown in Fig. 3(a) is rotated at an angle (90°–*i*) with the vertical axis, as has been illustrated in Fig 3(b). The stresses acting along the vertical and horizontal planes (Eqs. (8)-(10)) are used to calculate the stresses on the plane parallel to the sloping surface using the stress transformation.

The value of transformed stress $\sigma_{v\,(90^\circ-i)}$ acting along $x_{(90^\circ-i)}\,y_{(90^\circ-i)}$ coordinates can be given as

$$\sigma_{v(90^\circ-i)} = \sigma_h \sin^2(90^\circ - i) + \sigma_v \cos^2(90^\circ - i) - 2\tau_{vh} \sin(90^\circ - i)\cos(90^\circ - i) \quad (11)$$

or

$$\sigma_{v(90^\circ-i)} = \sigma_h \cos^2(i) + \sigma_v \sin^2(i) - 2\tau_{vh} \cos(i)\sin(i) \quad (12)$$

Substituting Eqs. (8), (9) and (10) into Eq. (12) yields the stress $\sigma_{v\,(90^\circ-i)R}$ at the depth *z* as

$$\sigma_{v(90^\circ-i)R} = K\sigma_v \cos^2(i) + \sigma_v \sin^2(i) - (c + K\sigma_v \tan\phi)(\sin 2i) \quad (13)$$

It needs to be noted here that an assumption of vertical and horizontal principal stresses was made by Marston and Anderson (1913) and Terzaghi (1943) when the value of lateral stress ratio *K* was suggested to be equal to the active Rankine ratio. However, for the case when the principal stresses are not vertical and horizontal, Landanyi and Hoyaux (1969) used the concept of stress transformation to provide an alternate expression for the lateral stress ratio *K*,

$$K = \frac{\cos^2\phi}{1+\sin^2\phi} \quad (14)$$

In Fig. 2, the force $F_{v\,(90^\circ-i)R}$ acting on *dz* is given as

$$F_{v(90^\circ-i)R} = \left\{K\sigma_v \cos^2(i) + \sigma_v \sin^2(i) - (c + K\sigma_v \tan\phi)(\sin 2i)\right\}dz \quad (15)$$

The horizontal component of the force $F_{v\,(90^\circ-i)R}\cos i$ acting normal to *dz* can be determined as

$$F_{v(90^\circ-i)R}\cos i = \left\{K\sigma_v \cos^2(i) + \sigma_v \sin^2(i) - (c + K\sigma_v \tan\phi)(\sin 2i)\right\}dz\cos i \quad (16)$$

Using Eq. (16), the horizontal stress $\sigma_{v\,(90^\circ-i)R}\cos i$ acting normal to *dz* can be given as

$$\sigma_{v(90^\circ-i)R}\cos i = \left\{K\sigma_v \cos^2(i) + \sigma_v \sin^2(i) - (c + K\sigma_v \tan\phi)(\sin 2i)\right\}\cos i \quad (17)$$

Hence the shear stress τ_R acting on *dz* along the shear plane *RS* can be obtained as

$$\tau_R = c + \tan\phi\cos i\left\{K\sigma_v \cos^2(i) + \sigma_v \sin^2(i) - (c + K\sigma_v \tan\phi)(\sin 2i)\right\} \quad (18)$$

The value of shear force F_{sR} can be given as

$$F_{sR} = \left\{c(1 - \tan\phi\cos i\sin 2i) + \sigma_v \tan\phi\cos i\left\{K\cos^2(i) + \sin^2(i) - K\tan\phi\sin 2i\right\}\right\}dz \quad (19)$$

Similarly, along the shear plane *PQ*, the shear force F_{sL} acting on *dz* at a depth *z*+*B*tan*i* can be given as

$$F_{sL} = \left\{\begin{matrix} c(1 - \tan\phi\cos i\sin 2i) \\ + \tan\phi\cos i(\sigma_v + \gamma B\tan i)\left(K\cos^2(i) + \sin^2(i) - K\tan\phi\sin 2i\right)\end{matrix}\right\}dz \quad (20)$$

Considering the vertical equilibrium, the sum of the forces can be given as

$$(F_v + dF_v) + F_{sL} + F_{sR} = F_v + dW \quad (21)$$

Substitution of Eqs. (5), (6) (7), (19) and (20) into Eq. (21) yields

$$Bd\sigma_v + \left[\begin{matrix} 2c(1 - \tan\phi\cos i\sin 2i) \\ + (2\sigma_v + \gamma B\tan i)\left(\tan\phi\cos i\left\{K\cos^2(i) + \sin^2(i) - K\tan\phi\sin 2i\right\}\right)\end{matrix}\right]dz = \gamma B dz \quad (22)$$

Defining *N* as

$$N = \tan\phi\cos i\left\{K\cos^2(i) + \sin^2(i) - K\tan\phi\sin 2i\right\} \quad (23a)$$

Similarly defining *P* as

$$P = 1 - \tan\phi\cos i\sin 2i \quad (23b)$$

Replacing values from Eqs. (23a) and (23b) into Eq. (22) and solving

$$\frac{d\sigma_v}{dz} + \frac{2N}{B}(\sigma_v) = \gamma - \frac{2c}{B}(P) - \gamma N\tan i \quad (24)$$

Eq. (24) is a first-order differential equation, which can be rearranged as

$$\frac{d\sigma_v}{dz}\left(e^{2N\frac{z}{B}}\right) - \frac{2N}{B}(\sigma_v)\left(e^{2N\frac{z}{B}}\right) = \left[\gamma - \frac{2c}{B}(P) - \gamma NK\tan i\right]\left(e^{2N\frac{z}{B}}\right) \quad (25)$$

or

$$\int\frac{d\sigma_v}{dz}\left(e^{2N\frac{z}{B}}\right)dz = \int\left\{\left[\gamma - \frac{2c}{B}(P) - \gamma N\tan i\right]\left(e^{2N\frac{z}{B}}\right)\right\}dz \quad (26)$$

or

$$\sigma_v = B\left[\frac{\gamma(1 - N\tan i) - \frac{2c}{B}(P)}{2N}\right] + Ce^{-2N\frac{z}{B}} \quad (27)$$

where *C* is a constant of integration.

At *z*=0, with an assumption of uniform stress distribution

$$\sigma_v = q + \gamma\frac{B\tan i}{2} \quad (28)$$

For *z*=0, Eqs. (27) and (28) are equated to give

$$C = q + \gamma\frac{B\tan i}{2} - B\left[\frac{\gamma(1 - N\tan i) - \frac{2c}{B}(P)}{2N}\right] \quad (29)$$

Substituting the value of *C* from Eq. (29) into Eq. (27)

$$\sigma_v = \gamma B\left\{\left[\frac{1 - N\tan i - \frac{2c}{\gamma B}(P)}{2N}\right]\left(1 - e^{-2N\frac{z}{B}}\right) + \left(\frac{q}{\gamma B} + \frac{\tan i}{2}\right)e^{-2N\frac{z}{B}}\right\} \quad (30)$$

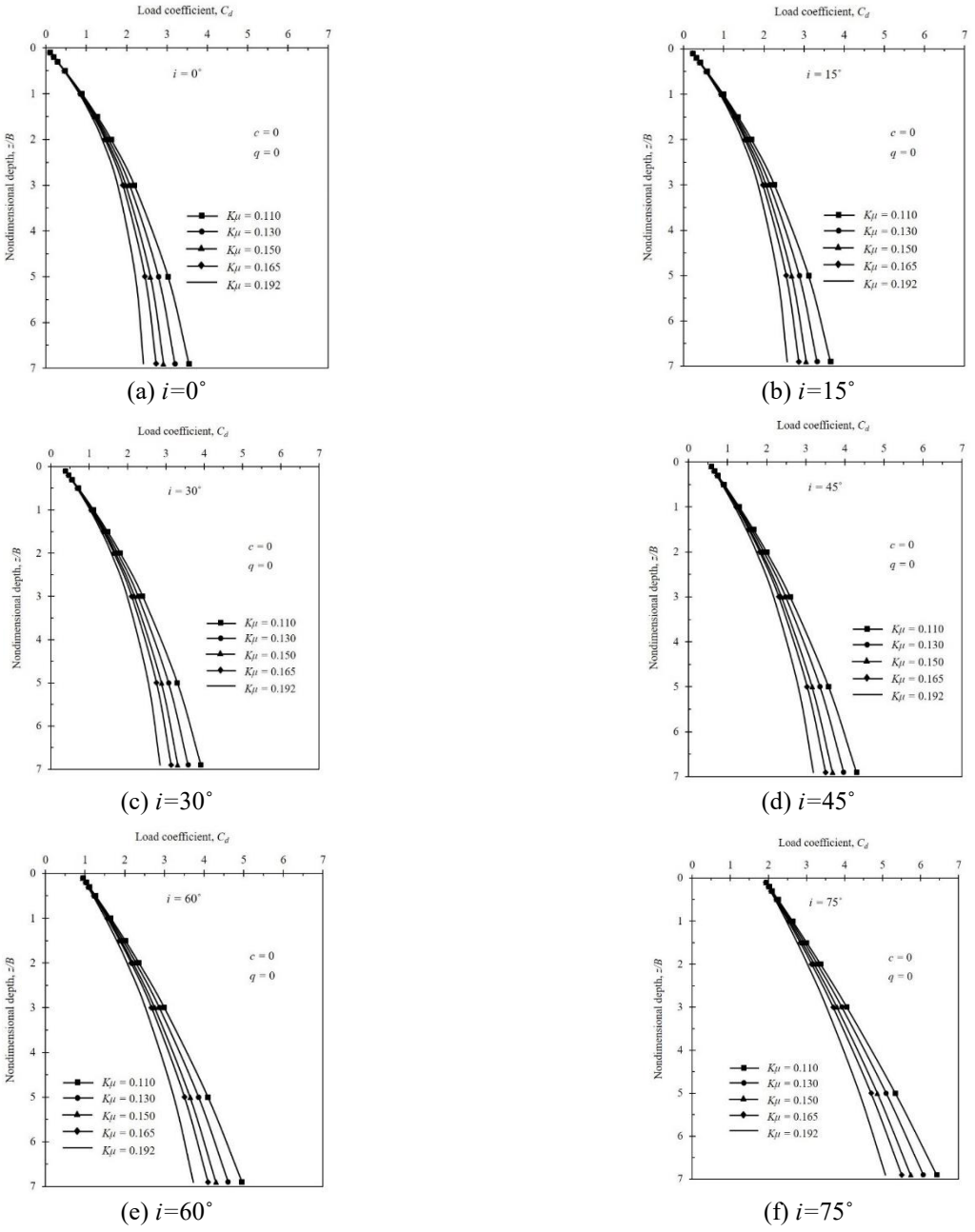

(a) i=0˚ (b) i=15˚

(c) i=30˚ (d) i=45˚

(e) i=60˚ (f) i=75˚

Fig. 4 Variation of load coefficient with nondimensional depth for typical arching factor values

Using Eq. (30), vertical load W on the rigid conduit of diameter B_c buried in soil slope is given as

$$W = \sigma_v B = \gamma B^2 \left\{ \left[\frac{1 - N\tan i - \frac{2c}{\gamma B}(P)}{2N} \right] \left(1 - e^{-2N\frac{z}{B}} \right) + \left(\frac{q}{\gamma B} + \frac{\tan i}{2} \right) e^{-2N\frac{z}{B}} \right\} \quad (31)$$

whereas, vertical load W on a flexible conduit is obtained by multiplying Eq. (31) with B_c/B

$$W = \gamma B B_c \left\{ \left[\frac{1 - N\tan i - \frac{2c}{\gamma B}(P)}{2N} \right] \left(1 - e^{-2N\frac{z}{B}} \right) + \left(\frac{q}{\gamma B} + \frac{\tan i}{2} \right) e^{-2N\frac{z}{B}} \right\} \quad (32)$$

Eqs. (31) and (32) can be simplified as Eqs. (1) and (2), where load coefficient C_d is given as

$$C_d = \left[\frac{1 - N\tan i - \frac{2c}{\gamma B}(P)}{2N} \right] \left(1 - e^{-2N\frac{z}{B}} \right) + \left(\frac{q}{\gamma B} + \frac{\tan i}{2} \right) e^{-2N\frac{z}{B}} \quad (33)$$

For different conditions of surcharge, soil, and slope angle, the value of load coefficient C_d can be obtained by using Eq. (33). For q=0, c=0 and i=0˚

$$C_d = \frac{1}{2K\mu} \left(1 - e^{-2K\mu\frac{z}{B}} \right) \quad (34)$$

Eq. (34) is the same expression as presented by Marston

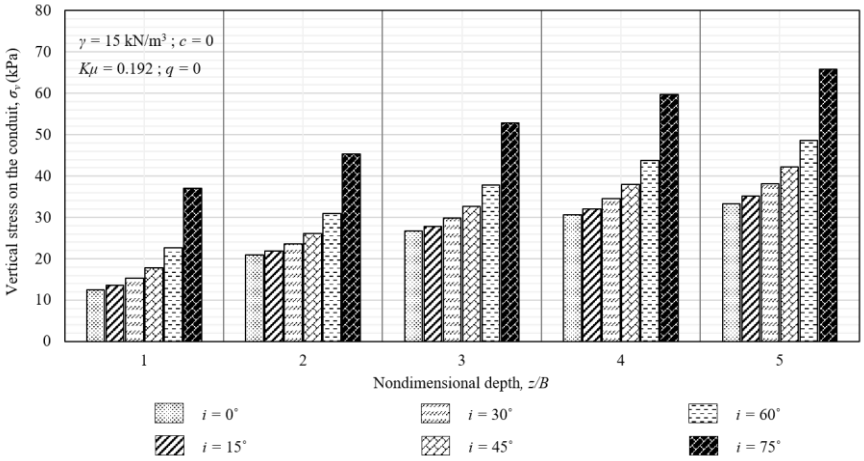

Fig. 5 Effect of slope angle on the vertical stress on the conduit

and Anderson (1913), Terzaghi (1943), and Spangler (1962) for conduits buried under the level ground. With all its assumptions and limitations, this equation is still one of the most commonly used expressions to estimate the vertical load on conduits buried under a level ground surface.

3. Results and discussion

In the present study, the analytical expression has been formulated to calculate the vertical load on a conduit buried under the sloping ground. The load coefficient C_d, provided in Eq. (33) can be used to understand the effect of the arching phenomenon on the vertical load estimation for the conduit buried under a sloping surface, inclined at various slope angles.

Fig. 4 illustrates the variation of load coefficient C_d with non-dimensional depth z/B, as the design charts for slope angles i=0˚, 15˚, 30˚, 45˚, 60˚ and 75˚. Typical arching factor $K\mu$ values for different soils have been considered, as provided in Table 1 (Spangler and Handy 1973, Greenwood and Lang 1990, Moser and Folkman 2001).

Other specific values of parameters used are q=0 and c=0. It is observed that for all values of i, C_d increases nonlinearly with an increase in z/B for all $K\mu$ values. Moreover, it is also noted that at lower values of z/B, the curves for various types of soil are not very different. This shows that at shallow depths, the type of soil does not affect the amount of load reaching the conduit. However, at higher depths, the maximum and minimum C_d values are observed for the saturated clay and noncohesive soil, respectively.

Table 1 Typical arching factor values for different soils

Type of soil	Arching factor
Saturated clay	0.110
Ordinary clay	0.130
Saturated topsoil	0.150
Sand, gravel	0.165
Non-cohesive	0.192

This shows that for greater burial depths, the amount of load reaching the conduit is a function of the type of overlaying soil. As compared to the noncohesive soil, more vertical load will reach the conduit that is buried under the saturated clay. Similar conclusions were drawn by Spangler and Handy (1973) and Greenwood and Lang (1990) for the conduits buried under the level ground (i.e., i=0˚). It is also noted that for any type of soil, an increase in slope angle i results in an increase in the load coefficient C_d for any z/B value.

In order to better explain this fact, Fig. 5 is provided to illustrate the effect of slope angle i on the vertical stress on the conduit σ_v, buried under noncohesive soil i.e., $K\mu$ = 0.192, for different values of the nondimensional depth z/B. Other specific values of various used parameters are γ=15kN/m^3, q=0 and c=0. It is observed that for all values of z/B, an increase in i results in a nonlinear increase in the value of σ_v. For all z/B values, the minimum increase is noted when the slope angle i increases from 0˚ to 15˚ and the maximum increase is observed as the value of i increases from 60˚ to 75˚. On average, a 15-degree increment in the value of the slope angle results in increasing the value of the vertical stress on the conduit by 17.71%.

The effect of soil arching on the vertical load on the conduit may be expressed quantitatively in terms of the ratio of vertical stress on the conduit to the overburden pressure, called the arching ratio A (Mcnulty 1965, Al-Naddaf *et al.* 2017). It is defined as

$$A = \left(\frac{q^* - \sigma_v}{q^*} \right) \times 100 \tag{35}$$

where $q^*=\gamma(z+B\tan i)+q$

Fig. 6 shows the variation of arching ratio A with the applied surface pressure q at different nondimensional depths z/B and slope angles i, for the specific values of the parameters as γ=15 kN/m^3, ϕ=30˚ and c=0. It can be seen that irrespective of the value of i, q does not have any significant effect on A at lower values of z/B. However, at higher z/B values, a noticeable effect of the increase in q can be observed on the value of A. This is in line with the

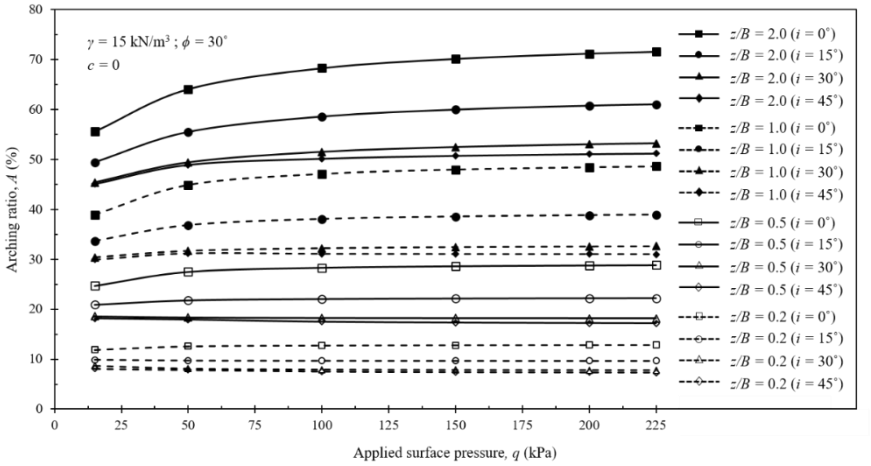

Fig. 6 Variation of surface surcharge with the arching ratio

previous observations that the effect of the arching phenomenon on the vertical load on a buried conduit is insignificant when the conduit is buried at lower depths and increases with an increase in burial depth. Similar observations were also made by Getzler *et al.* (1968) while studying the effect of arching on vertical load on structures buried under a poorly graded quartz sand, having a level surface (i.e., i=0˚). Moreover, it is also noticed that for any value of z/B, the arching ratio A is maximum when the conduit is buried under the level ground (i.e., i=0˚). However, an increase in the slope angle i results in reducing the value of A. This shows that under the application of a surface surcharge, the amount of vertical stress reaching the conduit buried under a sloping ground is more as compared to the conduit buried under the level ground. On average, a 15-degree increment in the value of the slope angle results in decreasing the value of arching ratio by 19.08%.

4. Numerical analysis through finite element method

The analytical results have also been compared with a finite element model (FEM) that was developed using commercial software, PLAXIS 2D (2016). It is a very helpful tool for conducting finite element analysis to study complex soil-structure interaction (Fan and Luo 2008).

4.1 Soil model

PLAXIS 2D software has various models to simulate the soil behavior. In this study, the hardening soil model was used because it is the true second-order model and can generally be used for all types of applications. It is also considered to provide accurate results for the problems that involve mobilization of the shear strength e.g., tunnel construction projects (Brinkgreve and Vermeer 2002). The hardening soil model requires 10 input parameters, namely total unit weight of soil γ, reference stress p^{ref}, reference stiffness parameter for triaxial compression E_{50}^{ref}, reference stiffness parameter for oedometer loading E_{oed}^{ref}, reference stiffness parameter for triaxial unloading E_{ur}^{ref}, Poisson's ratio of unloading and reloading ν_{ur}, power for stress-dependent stiffness m, friction angle ϕ, cohesion c, and dilatancy angle ψ. Brinkgreve (2005) has suggested that for sandy soils, the value of E_{50}^{ref} at p^{ref}=100 kPa ranges between 15 MPa for loose sand to 50 MPa for dense sand. Schanz (1998) has suggested that while E_{oed}^{ref}= E_{50}^{ref}, the value of E_{ur}^{ref} = 3-5 times E_{50}^{ref}. The values of power for stress-dependent stiffness m and the Poisson's ratio of unloading and reloading ν_{ur} range between 0.4-0.7 and 0.10-0.25, respectively. The selected parameters used for the analysis were based on the aforementioned guidelines and are provided in Table 2.

Table 2 Soil parameters used in the FE model

Soil parameter	Unit	Value
E_{50}^{ref}	MPa	40
E_{oed}^{ref}	MPa	40
E_{ur}^{ref}	MPa	160
p^{ref}	kPa	100
m	-	0.7
ν_{ur}	-	0.2
γ	kN/m^3	20
c	kPa	5
ϕ	degree	30

4.2 Conduit

The conduit was modeled using a tool called "tunnel designer", which generates the plate element segments to form a circular structure. The properties of plate elements of the tunnel are represented in terms of stiffness parameters namely, normal stiffness EA, flexural rigidity EI and Poisson's ratio ν. In order to get a better understanding of the effect of stiffness on the vertical load estimation, both rigid corrugated steel (CS) and flexible high-density polyethylene (HDPE) conduits were analyzed. It needs to be mentioned here that the corrugation geometry of the CS conduit was not modeled explicitly, rather EA and EI values were used (Wadi *et al.* 2015). The set of parameters for the

Table 3 Stiffness parameters of conduit materials used in the FE model

Conduit material	Parameter				
	B_c	t	EA	EI	v_c
	m	m	kN/m	kNm^2/m	-
Corrugated steel (CS)	2.0	60.02×10^{-3}	7.0×10^5	211.5	0.28
High density polyethylene (HDPE)	2.0	63.26×10^{-3}	4.2×10^3	1.4	0.46

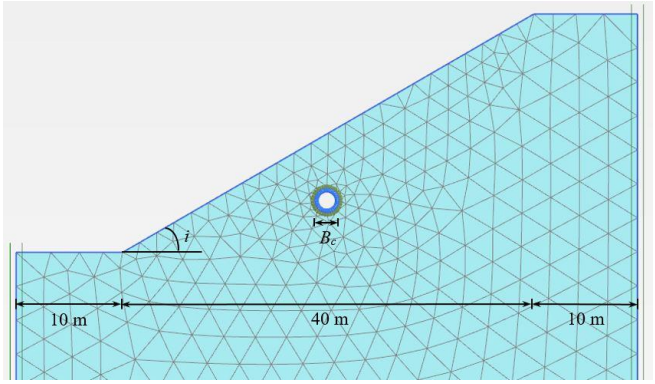

Fig. 7 FE model of the conduit buried under the sloping ground

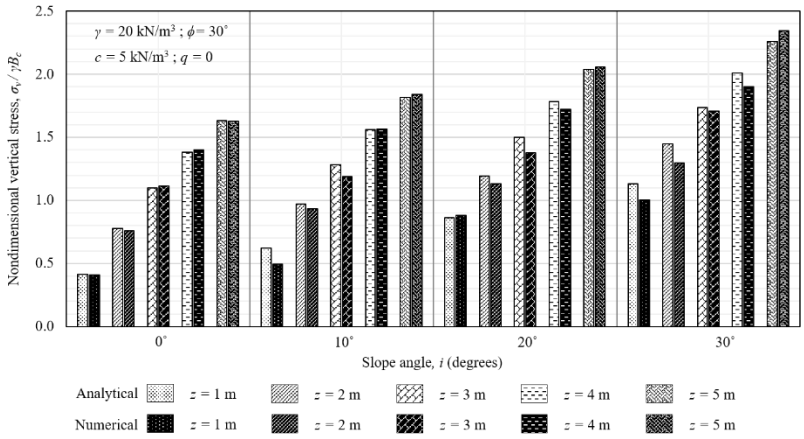

Fig. 8 Comparison of analytical and numerical results for the nondimensional vertical stress on CS conduit

material used are based on the parameters defined by Elshimi and Moore (2013), as given in Table 3. Interface elements were employed to simulate the interaction between the conduit and the surrounding soil. To account for a realistic frictional resistance between the conduit and the adjacent soil, the value of the strength interaction parameter R_{inter} was taken as 0.8 (Wadi *et al.* 2015).

4.3 Methodology

At first, both CS and HDPE conduits were analyzed under the level ground (i.e., i=0˚). Thereafter, soil slopes with angle i=10˚, 20˚ and 30˚ were modeled for analyzing the effect of slope angle on the vertical stress on the crown of the conduit. Standard fixities were applied automatically to the boundaries of the model. For an exclusive study of the effect of slope surface, the conduit was installed in a manner that slope berms were kept away from the center of the installed conduit by≈10 times its diameter, as shown in Fig. 7. This also helped in minimizing the effect of boundary conditions on stress distribution within the soil model and around the conduit. For obtaining accurate numerical results, the fine mesh size was used for the analysis. In the preliminary phase of the numerical modeling, the initial state of stress of the model for the level ground (i.e., i=0˚) was evaluated by considering the K_0 procedure option. Whereas, the initial stress of the model for the sloping ground (i.e., i=10˚, 20˚, and 30˚) was evaluated by considering the gravity loading option. In the following phase, the state of stress for all values of slope angle i weas studied by conducting the plastic analysis. During the numerical investigation, the depth of the crown of the buried conduit from the surface of soil slope was increased and the value of vertical stress σ_v on the crown of the conduit was extracted.

4.4 Comparison of analytical results with numerical findings

Fig. 8 illustrates the comparison of the values of

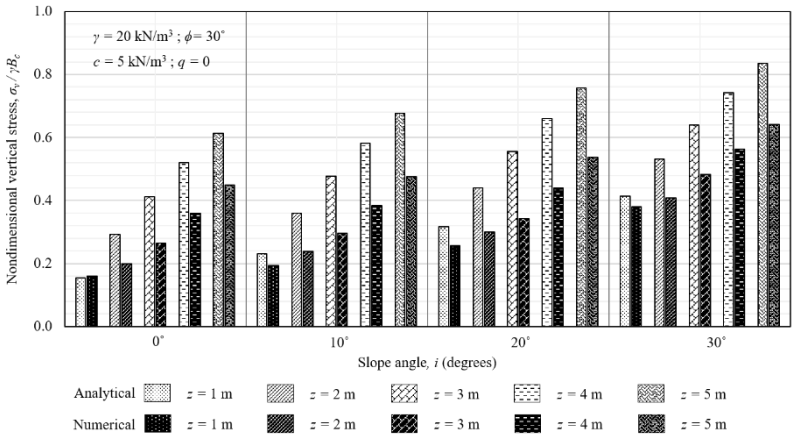

Fig. 9 Comparison of analytical and numerical results for the nondimensional vertical stress on HDPE conduit

nondimensional vertical stress $\sigma_v/\gamma B_c$ on the crown of the conduit, calculated using the developed analytical expression (Eq. (31)) with the values extracted from the developed numerical model for the CS conduit. The specific values of other parameters are γ=20 kN/m^3, ϕ=30°, c=5 kPa, and q=0. As expected, due to higher stiffness negative arching is observed to occur for the CS conduit, where the width of the overburden soil prism is greater than the diameter of the buried conduit. Through iterations, it was determined that the conduit takes the load of the overburden soil prism of width B=5.5 m. The values of the nondimensional vertical stress $\sigma_v/\gamma B_c$ at various depths z for i=0° correspond to Eq. (1), which was given by Spangler (1962) for estimating the vertical load on a rigid conduit buried under the level ground. It is also observed that for both analytical and numerical results, the nondimensional vertical stress $\sigma_v/\gamma B_c$ increases with an increase in the slope angle i. On average, a 10-degree increment in slope angle increases the value of $\sigma_v/\gamma B_c$ by 19.87% for the analytical expression (Eq. (31)) and 21.28% for the developed numerical model. This shows that the results obtained using the analytical expression and the numerical model are in good agreement, with a maximum deviation of 6.98%.

Fig. 9 illustrates the comparison of the values of nondimensional vertical stress $\sigma_v/\gamma B_c$ on the crown of the conduit, calculated using the developed analytical expression (Eq. (32)) with the values achieved from the developed numerical model for the HDPE conduit. The specific values of other parameters are γ=20 kN/m^3, ϕ=30°, c=5 kPa, and q=0. It is observed that all the values of $\sigma_v/\gamma B_c$ are below 1.0, presenting the occurrence of positive arching for the HDPE conduit. This happens due to the fact that because of the lower stiffness of the conduit material, the load of the overburden soil prism is not taken by the buried conduit. Rather it is spread over the entire width of the soil prism, resulting in decreasing the amount of vertical load on the conduit (Spangler 1962, Spangler and Handy 1973). The values of nondimensional vertical stress $\sigma_v/\gamma B_c$ at various depths z for i=0° correspond to Eq. (2), which was given by Spangler (1962) for estimating the vertical load on a flexible conduit buried under the level ground. It is also noted that when compared to the results extracted from the numerical model, the results calculated using the analytical expression overestimate the value of $\sigma_v/\gamma B_c$ by approx. 19%. This shows that Spangler's expression (Eq. (2)) and the developed analytical expression (Eq. (32)) not only help in achieving a more economical design when compared with the rigid conduit, but also ensure the safety of the flexible conduit. Furthermore, it is also observed that for both analytical and numerical results, the nondimensional vertical stress $\sigma_v/\gamma B_c$ increases with an increase in the slope angle i. On average, a 10-degree increment in slope angle increases the value of $\sigma_v/\gamma B_c$ by 19.87% for the analytical expression (Eq. (32)) and 25.76% for the developed numerical model. This shows that the results obtained using the analytical expression and the numerical model are in good agreement, with a maximum deviation of 11.61%.

Wadi *et al.* (2015) used PLAXIS 2D software to study the effect of slope angle on the maximum normal stress on the corrugated steel (CS) pipe culverts of different diameters, buried under the sloping ground. The maximum normal stress, extracted from FE modeling can be used to ensure the safe design of a buried conduit. Since the vertical stress σ_v is the contact stress normal to the crown of the buried conduit, it can also be compared with the values of maximum normal stress σ_n obtained using the PLAXIS 2D software. Fig. 10 illustrates the comparison of the nondimensional normal stress $\sigma_n/\gamma B_c$ on the conduit, calculated using the developed analytical expression (Eq. (31)) with the values extracted from the developed numerical model and the average results of Wadi *et al.* (2015), for different burial depths z and slope angles i. The values of the normal stress on the conduit achieved using PLAXIS 2D for the developed numerical model and the results of Wadi *et al.* (2015) are the maximum absolute values of the normal stress extracted from the commercial software. It is observed that the results achieved from the developed expression are in good agreement with the results extracted from the numerical models (developed and Wadi *et al.* 2015) with an average deviation of about 17%. This difference is more when the value of slope angle i is lower (< 20°), but reduces significantly for the higher values of the i. This is also supported by the results of the maximum deformation of the CS pipe culverts, presented by Wadi *et al.* (2015) that show that with an increase in the slope angle, the location of the maximum deformation of the pipe

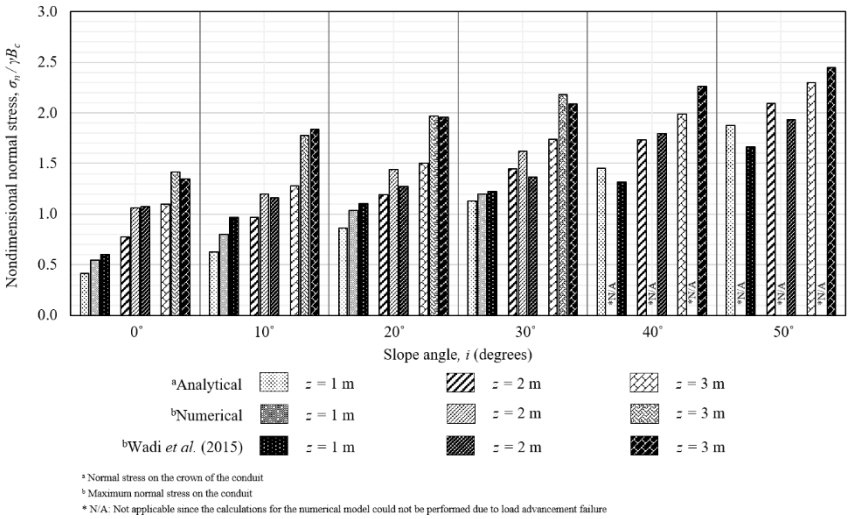

Fig. 10 Comparison of the analytical results with the numerical results extracted from the developed FE model and Wadi *et al.* (2015), for nondimensional normal stress on the CS conduit

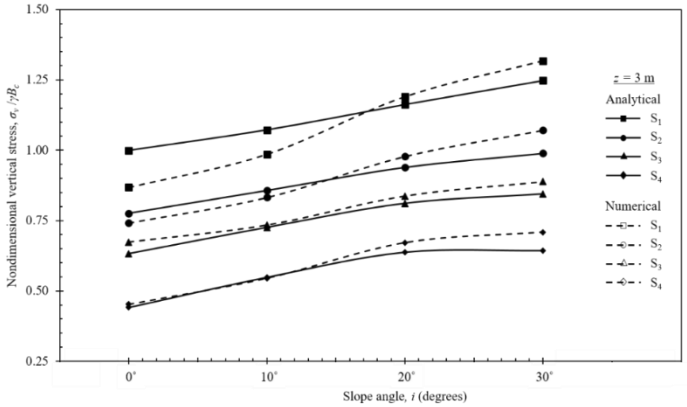

Fig. 11 Comparison of the analytical results with the numerical results for different sandy soils

ulvert gradually concentrates towards its crown. Furthermore, it is also noted that for both analytical and numerical results, the nondimensional normal stress $\sigma_n/\gamma B_c$ increases with an increase in the slope angle i. On average, a 10-degree increment in slope angle increases the value of $\sigma_n/\gamma B_c$, obtained from the developed analytical expression, the developed numerical model, and Wadi *et al.* (2015) by 24.50%, 20.53%, and 16.68%, respectively. Thus, it can be said that the developed analytical expression is a good and dependable alternative to the expensive commercial software to calculate the value of the design stress that the conduit may experience upon its burial under the sloping ground.

The general validity of the developed analytical expression was checked by comparing the analytically calculated results with the numerically simulated results for the vertical stress on the corrugated steel (CS) conduit, when buried under different types of soil. The soil parameters presented in Table 4 are considered to be representative of most sandy soils (Ghazavi and Eghbali 2008, Moayedi *et al.* 2020).

By using the same method as described above, the vertical stress σ_v on the CS conduit was obtained from the

Table 4 Soil parameters representative of most common sandy soils

Soil type	Soil No.	Soil parameters				
		γ	E_s	ϕ	ψ	υ_s
		(kN/m^3)	MPa	degree	degree	-
Loose sand	S_1	19.0	17.5	30	3.4	0.333
Medium dense sand	S_2	20.1	27.5	34	6.4	0.306
Dense sand	S_3	20.7	40.0	37	8.8	0.285
Very dense sand	S_4	21.1	65.0	42	11.5	0.249

analytical expression and the developed numerical model. Fig. 11 illustrates the comparison of the nondimensional vertical stress $\sigma_v/\gamma B_c$ on the conduit, calculated using the developed analytical expression (Eq. (31)) with the values extracted from the developed numerical model for different soil types (S_1 – S_4) and slope angles i. The burial depth of the conduit was taken as z=3 m. It can be observed that for both analytical and numerical results, the nondimensional vertical stress $\sigma_v/\gamma B_c$ increases with an increase in the slope angle i. On average, a 10-degree increment in the slope angle increases the value of $\sigma_v/\gamma B_c$ by 13.77% for the

analytical expression and 16.39% for the developed numerical model. Furthermore, it can also be noted that the analytically obtained results are in good agreement with the numerically simulated results, with a maximum deviation of 9.81%. The congruence of the results shows that the applicability of the developed analytical expression is not limited to a specific set of soil parameters, and can generally be used for different types of soil.

5. Conclusions

On the basis of the details presented in the previous sections, the following conclusions can be drawn:

a) The generalized analytical expression developed for the vertical load on a conduit buried under the sloping ground incorporates the effect of slope angle and soil arching.

b) At any known depth below the sloping ground, an increase in slope angle causes an increase in the load coefficient, resulting in an increase in the vertical load on the buried conduit.

c) The amount of load reaching the conduit is a function of the type of overlaying soil. An increase in the arching factor causes a decrease in the load coefficient, resulting in a decrease in the vertical load on the buried conduit.

d) An increase in the slope angle reduces the effect of the arching phenomenon on the vertical load on a buried conduit. As a result, the conduit buried under the sloping ground is subject to a higher value of vertical load as compared to the conduit buried under the level ground.

e) The values of the vertical load calculated using the developed expression can be used satisfactorily for the purpose of the design of the conduit. The design charts presented here for the cohesionless soil slope, without any surcharge can be used routinely by practicing engineers. For any generalized case, the analytical expression can be used, and if required new design charts can also be prepared for simple cases using the developed expression, without depending on complex and expensive analyses/software.

f) The analytical expression can be used effectively to provide a good estimation of the vertical load on both rigid and flexible conduits, buried in the ditch condition. The developed expression can be extended further to incorporate the effect of varying degrees of the stiffness of different conduit materials and embankment types using Marston/Spangler's theory of plane of equal settlement/ settlement ratio.

Acknowledgments

This research was funded by The Higher Education Commission, Government of the Islamic Republic of Pakistan.

Data availability statement

All data, models, and code generated or used during the study appear in the submitted article.

References

Al-Naddaf, M., Han, J., Jawad, S., Abdulrasool, G. and Xu, C. (2017), "Investigation of stability of soil arching under surface loading using trapdoor model tests", *Proceedings of the 19th International Conference on Soil Mechanics and Geotechnical Engineering*, Seoul, South Korea, September.

Allard, E. and El Naggar, H. (2016), "Pressure distribution around rigid culverts considering soil-structure interaction effects", *Int. J. Geomech.*, **16**(2), 04015056. https://doi.org/10.1061/(ASCE)GM.1943-5622.0000525.

Alzabeebee, S., Chapman, D.N. and Faramarzi, A. (2018), "Innovative approach to determine the minimum wall thickness of flexible buried pipes", *Geomech. Eng.*, **15**(2), 755-767. https://doi.org/10.12989/gae.2018.15.2.755.

Atkinson, J. (2007), *The Mechanics of Soils and Foundations*, (2nd Edition), Taylor and Francis, New York, U.S.A.

Aysen, A. (2002), *Soil Mechanics: Basic Concepts and Engineering Applications*, Taylor and Francis, New York, U.S.A.

Bjerrum, L., Frimann, L.J., Has, M. and Duncan, J.M. (1972), "Earth pressures on flexible structures (state of the art report)", *Proceedings of the 5th European Conference on Soil Mechanics and Foundation Engineering*, Madrid, Spain, April.

Brinkgreve, R.B. and Vermeer, P.A. (2002), *Plaxis User's Manual-Version 8.2*, Delft University of Technology and Plaxis bv, Delft, The Netherlands.

Brinkgreve, R.B. (2005), "Selection of soil models and parameters for geotechnical engineering application", *Proceedings of the Geo-Frontiers Congress*, Austin, Texas, U.S.A., January.

Bryden, P., El Naggar, H. and Valsangkar, A. (2015), "Soil-structure interaction of very flexible pipes: Centrifuge and numerical investigations", *Int. J. Geomech.*, **15**(6), 04014091. https://doi.org/10.1061/(ASCE)GM.1943-5622.0000442.

Burghignoli, A. (1981), "Soil interaction in buried structures", *Proceedings of the 10th International Conference on Soil Mechanics and Foundation Engineering*, Stockholm, Sweden, June.

Chelapati, C.V. (1964), "Arching in soil due to the deflection of a rigid horizontal", *Proceedings of the Symposium on Soil-Structure Interaction*, Tuscon, Arizona, U.S.A., June.

Das, B.M. (2008), *Advanced Soil Mechanics*, (3rd Edition), Taylor and Francis, New York, U.S.A.

Dhar, A.S., Moore, I.D. and McGrath, T.J. (2004), "Two-dimensional analyses of thermoplastic culvert deformations and strains", *J. Geotech. Geoenviron. Eng.*, **130**(2), 199-208. https://doi.org/10.1061/(ASCE)1090-0241(2004)130:2(199).

Elshimi, T.M. and Moore, I.D. (2013), "Modeling the effects of backfilling and soil compaction beside shallow buried pipes", *J. Pipeline Syst. Eng. Pract.*, **4**(4), 04013004. https://doi.org/10.1061/(ASCE)PS.1949-1204.0000136.

Fan, C.C. and Luo, J.H. (2008), "Numerical study on the optimum layout of soil-nailed slopes", *Comput. Geotech.*, **35**(4), 585-599. https://doi.org/10.1016/j.compgeo.2007.09.002.

Getzler, Z., Komornik, A. and Mazurik, A. (1968), "Model study on arching above buried structures", *J. Soil Mech. Found. Div.*, **94**(5), 1123-1141.

Ghazavi, M. and Eghbali, A.H. (2008), "A simple limit equilibrium approach for calculation of ultimate bearing capacity of shallow foundations on two-layered granular soils", *Geotech. Geol. Eng.*, **26**, 535-542. https://doi.org/10.1007/s10706-008-9187-2.

Greenwood, M. and Lang, D. (1990), *Vertical Deflection of Buried Flexible Pipes*, in *Buried Plastic Pipe Technology, ASTM International*, West Conshohocken, Pennsylvania, U.S.A.

Kang, J., Parker, F., Kang, Y.J. and Yoo, C.H. (2008), "Effects of frictional forces acting on sidewalls of buried box culverts", *Int.*

J. Numer. Anal. Meth. Geomech., **32**(3), 289-306. https://doi.org/10.1002/nag.628.

Katona, M.G. (2017), "Influence of soil models on structural performance of buried culverts", *Int. J. Geomech.*, **17**(1), 04016031. https://doi.org/10.1061/(ASCE)GM.1943-5622.0000684.

Khan, M.U.A. and Shukla, S.K. (2020), "Load-settlement response and bearing capacity of a surface footing located over a conduit buried within a soil slope", *Int. J. Geomech.*, **20**(10), 04020173. https://doi.org/10.1061/(ASCE)GM.1943-5622.0001807.

Khatri, D.K., Han, J., Corey, R., Parsons, R.L. and Brennan, J.J. (2015), "Laboratory evaluation of installation of a steel-reinforced high-density polyethylene pipe in soil", *Tunn. Undergr. Sp. Tech.*, **49**, 199-207. https://doi.org/10.1016/j.tust.2015.04.013.

Kim, K.Y., Lee, D.S., Cho, J., Jeong, S.S. and Lee, S. (2013), "The effect of arching pressure on a vertical circular shaft", *Tunn Undergr. Sp. Tech.*, **37**, 10-21. https://doi.org/10.1016/j.tust.2013.03.001.

Ladanyi, B. and Hoyaux, B. (1969), "A study of the trap-door problem in a granular mass", *Can. Geotech. J.*, **6**(1), 1-14. https://doi.org/10.1139/t69-001.

Lambe, T.W. and Whitman, R.V. (1969), *Soil Mechanics*, John Wiley and Sons, New York, U.S.A.

Lee, I.M., Kim, D.H., Kim, K.Y. and Lee, S.W. (2016), "Earth pressure on a vertical shaft considering the arching effect in c-ϕ soil", *Geomech. Eng.*, **11**(6), 879-896. https://doi.org/10.12989/gae.2016.11.6.879.

Luscher, U. and K. Hoeg (1964), "The beneficial action of the surrounding soil on the load-carrying capacity of buried tubes", *Proceedings of the Symposium on Soil-Structure Interaction*, Tucson, Arizona, U.S.A., September.

Marston, A. and Anderson, A.O. (1913), "The theory of loads on pipes in ditches, and tests of cement and clay drain tile and sewer pipe", Bulletin No. 31, Engineering Experiment Station, Iowa State College of Agriculture and Mechanic Arts, Ames, Iowa, USA.

Marston, A. (1930), "The theory of external loads on closed conduits in the light of the latest experiments", *Proceedings of the 9th Annual Meeting of the Highway Research Board*, Washington D.C., USA, December.

McNulty, J.W. (1965), "An experimental study of arching in sand", AEWES Report No. I-674, Corps of Engineers, Vicksburg, Mississippi, U.S.A.

Moayedi, H., Moatamediyan, A., Nguyen, H., Bui, X.N., Bui, D.T. and Rashid A.S.A. (2020), "Prediction of ultimate bearing capacity through various novel evolutionary and neural network models", *Eng. Comput.*, **36**, 671-687. https://doi.org/10.1007/s00366-019-00723-2.

Mohamedzein, Y.E. and Al-Aghbari, M.Y. (2016), "Experimental study of the performance of plastic pipes buried in dune sand", *Int. J. Geotech. Eng.*, **10**(3), 236-245. https://doi.org/10.1080/19386362.2015.1124508.

Moore, I.D. (2001), *Buried Pipes and Culverts*: *Geotechnical and Geoenvironmental Engineering Handbook*, Springer, Boston, Massachusetts, U.S.A.

Moradi, G. and Abbasnejad, A. (2015), "Experimental and numerical investigation of arching effect in sand using modified Mohr Coulomb", *Geomech. Eng.*, **8**(6), 829-844. https://doi.org/10.12989/gae.2015.8.6.829.

Moser, A.P. and Folkman, S.L. (2001), *Buried Pipe Design*, McGraw-Hill, New York, U.S.A.

Nielson, F.D. (1966), "Soil structure arching analysis of buried flexible structures", Ph.D. Dissertation, University of Arizona, Tuscon, Arizona, U.S.A.

Sadrekarimi, J. and Abbasnejad, A.R. (2010), "Arching effect in fine sand due to base yielding", *Can. Geotech. J.*, **47**(3), 366-374. https://doi.org/10.1139/T09-107.

Schanz, T. (1998), "Zur Modellierung des Mechanischen Verhaltens von Reibungsmaterialen [On modeling the mechanical behavior of friction materials]", Ph.D. Dissertation, Stuttgart Universität, Stuttgart, Germany.

Spangler, M.G. (1962), *Culverts and Conduit*, McGraw-Hill, New York, U.S.A.

Spangler, M.G. and Handy, R.L. (1973), *Soil Engineering*, (3rd Edition), Harper and Row Publishers, New York, U.S.A.

Srivastava, A. and Babu, G.S. (2011) "Deflection and buckling of buried flexible pipe-soil system in a spatially variable soil profile", *Geomech. Eng.*, **3**(3), 169-188. https://doi.org/10.12989/gae.2011.3.3.169.

Talesnick, M.L., Xia, H.W. and Moore, I.D. (2011), "Earth pressure measurements on buried HDPE pipe", *Geotechnique*, **61**(9), 721-732. https://doi.org/10.1680/geot.8.P.048.

Terzaghi, K. (1943), *Theoretical Soil Mechanics*, John Wiley and Sons, New York, U.S.A.

Terzi, N.U., Erenson, C. and Selcuk, M.E. (2015), "Geotechnical properties of tire-sand mixtures as backfill material for buried pipe installations", *Geomech. Eng.*, **9**(4), 447-464. https://doi.org/10.12989/gae.2015.9.4.447.

Ting, C.H., Shukla, S.K. and Sivakugan, N. (2011), "Arching in soils applied to inclined mine stopes", *Int. J. Geomech.*, **11**(1), 29-35. https://doi.org/10.1061/(ASCE)GM.1943-5622.0000067.

Uchida, T. (2004), "Clarifying the role of pipe flow on shallow landslide initiation", *Hydrol. Process.*, **18**(2), 375-378. https://doi.org/10.1002/hyp.5214.

Wadi, A., Pettersson, L. and Karoumi, R. (2015), "Flexible culverts in sloping terrain: Numerical simulation of soil loading effects", *Eng. Struct.*, **101**, 111-124. https://doi.org/10.1016/j.engstruct.2015.07.004.

Wu, T.H. (1996), "Soil strength properties and their measurement", Report No. 247; Transportation Research Board, USA.

Xiao, S., Yan, L. and Cheng, Z. (2011), "A method combining numerical analysis and limit equilibrium theory to determine potential slip surfaces in soil slopes", *J. Mountain Sci.*, **8**(5), 718-727. http://doi.org/10.1007/s11629-011-2070-2.

Xu, C., Zhang, X., Han, J. and Yang, Y. (2019), "Two-dimensional soil-arching behavior under static and cyclic loading", *Int. J. Geomech.*, **19**(8), 04019091. https://doi.org/10.1061/(ASCE)GM.1943-5622.0001482.

Young, W.C., Budynas, R.G. and Sadegh, A.M. (2002), *Roark's Formulas for Stress and Strain*, (7th Edition), McGraw-Hill, New York, U.S.A.

CC